J. Math. Biol. 40, 473–499 (2000)
Digital Object Identifier (DOI):
10.1007/s002850000033

Mathematical Biology

A.F. Jones · H.M. Byrne · J.S. Gibson · J.W. Dold

A mathematical model of the stress induced during avascular tumour growth

Received: 15 November 1999 / Published online: 5 May 2000

Abstract. In this paper a mathematical model is developed to describe the effect of nonuniform growth on the mechanical stress experienced by cells within an avascular tumour. The constitutive law combines the stress-strain relation of linear elasticity with a growth term that is derived by analogy with thermal expansion. To accommodate the continuous nature of the growth process, the law relates the rate of change of the stress tensor to the rate of change of the strain (rather than relating the stress to the strain directly). By studying three model problems which differ in detail, certain characteristic features are identified. First, cells near the tumour boundary, where nutrient levels and cell proliferation rates are high, are under compression. By contrast, cells towards the centre of the tumour, where nutrient levels are low and cell death dominant, are under tension. The implications of these results and possible model developments are also discussed.

1. Introduction

Advances in experimental technology (*e.g.* gene sequencing, fluorescent staining techniques) are enabling experimentalists to identify many physical mechanisms whose normal function is impaired in solid tumour growth. For example, populations of tumour cells which contain mutant versions of the gene p53 can survive under abnormally low oxygen tensions (*i.e.* hypoxia) [13]. Consequently the size of the hypoxic region in a tumour containing normal and mutant p53 cell populations will be larger than that in a tumour with only normal p53. Given that hypoxic cells progress slowly (if at all) through the cell cycle, anti-cancer therapies that target rapidly proliferating cells will be markedly less effective at reducing tumours containing mutant p53 than those with only wild-type p53.

The above description highlights the importance of genetic mutations in solid tumour growth. This is an area of active research in oncology. Other factors which have long been known to influence tumour growth are the supply of vital nutrients,

A.F. Jones, J.S. Gibson: Department of Mathematics, University of Manchester, Manchester M13 9PL, UK

H.M. Byrne: School of Mathematical Sciences, University of Nottingham, Nottingham NG7 2RD, UK. e-mail: etzhmb@thmech.nottingham.ac.uk

J.W. Dold: Department of Mathematics, UMIST, Manchester M60 1QD, UK

Key words: Tumour modelling – Stress – Elasticity – Growth

such as oxygen and glucose, and chemotherapeutic drugs [11], [17], [18], [33], [34].

More recent experimental results indicate that mechanical effects, such as stress, also play an important role in solid tumour growth [15]. By culturing multicellular spheroids in gels of increasing agarose concentration, Helmlinger *et al.* were able to demonstrate that increasing the stiffness of the embedding matrix (*i.e.* increasing the agarose concentration) reduced the limiting size of the tumour spheroids. Hence we deduce that stress fields generated in the matrix surrounding the tumour can inhibit cell growth. Equally, stress fields may be generated by cell growth or remodelling during cytokinesis [4]. Indeed, the main aim and novel aspect of this paper is the development of a mathematical model that describes the way in which nonuniform growth generate mechanical stress within a solid tumour. Such phenomena have not been widely studied in the mathematical literature. Instead, the majority of existing models have focussed either on the response of multicellular spheroids to changes in externally-delivered nutrients and chemotherapeutic treatments [1], [6], [14], [16], [20], [36] or on tumour angiogenesis [2], [5], [23], [31], the process by which tumours acquire a blood supply from their host tissue [10], [22], [24]. One notable exception is the paper by Chaplain and Sleeman [8] in which elasticity theory is used to describe tumour invasion. Problems associated with continuous growth in an elastic material are circumvented by modelling the tumour's outer proliferating rim as an elastic membrane of fixed volume. This rim surrounds an expanding core of necrotic, fluid-like material, *i.e.* tumour growth is assumed to correspond to growth of the necrotic core rather than an increase in the number of proliferating cells. Using linear stability analysis, they investigated the stability of the radially symmetric equilibrium configuration to asymmetric perturbations, arguing that invasion corresponded to growth of one or more of the perturbations.

Other models that incorporate mechanical effects include work by Drozdov and Khanina [9] and Skalak *et al.* [30]. For example, in [9] a simple example is discussed in which growth decouples from the underlying stress field and the corresponding growth-induced stress field is derived. Please and coworkers have developed an alternative model framework in which the tumour is treated as a multiphase medium, with cell growth, proliferation and death corresponding to appropriate phase changes between the water and cell phases [19], [26], [27].

Since the development of a mathematical model which couples together stress and growth would be extremely complex, in this paper we follow [9] and consider the simpler problem of growth-induced stress for which growth occurs independently of the underlying stress. Our approach builds directly upon existing models of solid tumour growth [1], [6], [14], [20], [36] in which cell growth and death are determined by levels of vital nutrients and are independent of mechanical effects such as stress. Such diffusion-limited growth models mimic the heterogeneous growth characteristic of multicellular spheroids, with cells near the nutrient-rich periphery proliferating rapidly whilst cells towards the centre of the tumour are starved of nutrients and consequently proliferate less rapidly, if at all [11], [17], [18], [33], [34].

A novel feature of the model presented in this paper concerns the development of an appropriate constitutive law that relates the differential growth within the

tumour to the mechanical stress experienced by the constituent cells. The constitutive law that we use combines the stress-strain relation of linear elasticity with a growth term that is derived by analogy with thermal expansion. Since proliferation and death are continuous processes, defined as rates, the constitutive law is stated in a dynamic fashion: it relates the rate of change of the stress tensor to the rate of change of the strain tensor, with a term present to describe the effect of the differential cell growth within the tumour. Similar laws have been proposed to describe the swelling of soft tissue being modelled as a multiphase poroelastic material [29].

The mathematical model that we develop is studied using a combination of numerical and asymptotic techniques for three situations of increasing complexity. First we study growth in a semi-infinite, smooth rectangular tube. We then consider growth in a finite, smooth rectangular tube before finally investigating growth of a radially-symmetric spherical tumour. Whilst the results obtained for each case differ in detail, several common features emerge. First, cells near the tumour boundary, where nutrient levels and cell proliferation rates are high, are under compression. By contrast, cells towards the centre of the tumour, where nutrient levels are low and cell death dominant, are under tension.

The remainder of the paper is organised as follows. In section 2 we present our mathematical model. In section 3 we study one-dimensional growth in a semi-infinite rectangular tube before considering growth in a finite tube in section 4. In section 5 attention focuses on the growth of a radially-symmetric tumour. The paper concludes in section 6 with a summary and discussion of the main results. An appendix describing the numerical method to construct the numerical solutions is also included.

2. The mathematical model

In this section we present a mathematical model that describes the development of an avascular tumour whose growth is regulated by an externally-supplied nutrient such as oxygen or glucose which diffuses freely throughout the tumour. Of particular interest is the way in which cell proliferation and cell death affect mechanical properties of the tumour such as stress. In the model the tumour is treated as a continuum, an approach which is valid when the tumour contains a sufficiently large number of cells that a small control volume (*i.e.* a region whose spatial scale is much less than that of the overall tumour) contains a large number of cells. Properties of the material at any point are then considered as average properties over a local region centred at that point. In particular, the elastic stresses in the tumour should be regarded as the average forces per unit area between adjoining *blocks* of tumour material, rather than as quantities determined by individual cell-to-cell interactions.

The key physical variables involved in the model are the nutrient concentration $c(\mathbf{r}, t)$, the tumour cell mass density $n(\mathbf{r}, t)$, the tumour cell velocity $\mathbf{v}(\mathbf{r}, t)$, the position of the tumour boundary $\Gamma(\mathbf{r}, t) = 0$, and the stress tensor $\boldsymbol{\sigma}(\mathbf{r}, t)$. Equations describing the evolution of these dependent variables are derived below, under the simplifying assumption that the tumour comprises proliferating cells only (*i.e.* it does not possess a central necrotic core).

As stated above, we assume that the key nutrient (henceforth 'the' nutrient) is supplied to the tumour from a well-stirred ambient environment and that, as it diffuses towards the centre of the tumour, it is consumed at a rate which is proportional to both the nutrient concentration and the tumour cell density. Following [1], [14], [20] and [36], we further assume that the nutrient evolves in a quasi-steady fashion. Combining these ideas, we deduce that the nutrient concentration $c(\mathbf{r}, t)$ satisfies the equation

$$0 = \underbrace{D_c \nabla^2 c}_{\text{diffusion}} - \underbrace{mcn/n^*}_{\text{consumption}}, \tag{1}$$

where D_c and m/n^* are the assumed constant diffusion coefficient and the nutrient consumption rate.

Turning now to the tumour cell density, we assume that the factors governing its evolution are cell proliferation, cell death (or apoptosis) [17], [18] and advection by a cell velocity $\mathbf{v}$. Thus, following [36], and in contrast to [25], [28], [35], we neglect random motility of the tumour cells. Assuming that the cell proliferation rate is proportional to both the cell density and the nutrient concentration and that the cell death rate is proportional to the cell density alone (*i.e.* tumour cells have a natural half-life), we deduce that the tumour cell density $n(\mathbf{r}, t)$ satisfies the equation

$$\frac{\partial n}{\partial t} + \nabla.(\boldsymbol{v}n) = (\alpha c - k)n, \tag{2}$$

where α and k are positive constants, related to the rates of cell proliferation and cell death. A number of assumptions are implicit in (2). Firstly we have assumed that other building materials, especially water which in practice constitutes the bulk of the cell mass, are freely available so that growth is controlled solely by nutrient availability. We further assume that the growth rate depends on the current amount of nutrient available and has no history dependence. We also assume that when a cell dies it dissipates instantaneously, converting entirely into water which is available for the production of new cells. While this is correct to leading order, there will be a small amount of nonutilisable debris whose large molecular size prevents it from diffusing away. Over a long period of time the accumulation of such material could produce a significant volume effect. For the model to be applicable at such times this effect would need to be incorporated [36].

Now the growth and death processes combine to establish the velocity $\mathbf{v}$ which describes cell movement as the tumour expands, or regresses, to accommodate the increase, or decrease, in the number of cells present. If we assume that the tumour cells have a constant density (*i.e.* the tumour mass per unit volume, rather than the number of cells, is constant), $n = n^*$, say, then equations (1) and (2) reduce to give the following scalar equations for the nutrient concentration $c(\boldsymbol{r}, r)$ and the cell velocity $\mathbf{v}(\boldsymbol{r}, t)$

$$0 = D_c \nabla^2 c - mc, \tag{3}$$

$$\nabla.\mathbf{v} = \alpha c - k, \tag{4}$$

and we no longer need to consider the tumour cell density explicitly.

A common feature of the simple geometries that are studied in this paper is one-dimensional growth. In such cases equation (4) is sufficient to determine the one, nonzero component of the velocity vector. In more general situations, with asymmetric growth, the continuity equation is coupled to the dynamics and constitutive equations, and cannot be solved separately. As an example of this, the tumour is modelled in [14] as a porous medium and Darcy's law is used to relate $\mathbf{v}$ to the pressure. Three additional equations are thus obtained which, together with equation (4), are sufficient to determine the cell velocity and the pressure.

We denote the tumour boundary by $\Gamma(\mathbf{r}, t) = 0$. Since this surface consists of tumour cells it must move with the cell velocity. Hence

$$\frac{D\Gamma}{Dt} \equiv \frac{\partial \Gamma}{\partial t} + (\mathbf{v}.\nabla)\Gamma = 0 \quad \text{on} \quad \Gamma = 0 \ , \tag{5}$$

where D/Dt represents the material derivative.

Since we are considering the tumour to be a continuum, the forces inside it can be represented by a stress tensor, $\boldsymbol{\sigma}$. If we assume further that growth is slow, and momentum changes are negligible, then the forces acting must be in balance at all times. There are no body forces, apart from gravity which we assume to be negligible, so our force balance yields

$$\nabla.\boldsymbol{\sigma} = \mathbf{0} \ . \tag{6}$$

Finally we formulate the constitutive law which relates the strain inside the tumour to the stress upon it. In doing this several basic assumptions are made. Firstly we assume that the tumour responds to stress in a purely elastic and isotropic fashion. Recall that we are not considering the forces between individual cells here but the average forces between blocks of material, each of which contain large numbers of cells. If tumours behave in the same way as other extensive biological tissues (*e.g.* ordinary flesh) then this is the simplest hypothesis to explain commonly observed behaviour, such as the fact that biological tissue stretches a finite amount when a force is imposed on it, but does not continue to deform indefinitely (this would be the response of a visco-elastic material). We further assume that the elastic response over any small time interval is proportional to the change in strain. Thus while the response is locally linear, the overall law is nonlinear because of convective effects and applies for large displacements. Another assumption is that there is no preferential direction for cell growth, so that growth produces isotropic strain. Finally, as stated above, we assume that the material is incompressible. Combining the above assumptions leads to the following equation

$$\underbrace{\frac{1}{2}\left(\nabla\mathbf{u} + \nabla\mathbf{u}^T\right)}_{\text{strain tensor}} = \underbrace{\frac{1}{3}g\boldsymbol{\delta}}_{\text{growth}} + \underbrace{\frac{1}{2E}(3\boldsymbol{\sigma} - \mathrm{Tr}(\boldsymbol{\sigma})\boldsymbol{\delta})}_{\text{stress response}}, \tag{7}$$

where $\mathbf{u}$ is the change in strain, g the volume per unit volume produced at a given point by growth, $\boldsymbol{\delta}$ is the Kronecker-delta ($\boldsymbol{\delta} = (\delta_{ij})$ where $\delta_{ij} = 1$ if $i = j$ and $\delta_{ij} = 0$ if $i \neq j$), Tr represents the trace of the tensor ($\mathrm{Tr}(\sigma) = \sum_{i=1}^{3} \sigma_{ii}$) and E is Young's modulus whose value will vary for different tumours. In the absence

of growth ($g = 0$), equation (7) reduces to the usual stress-strain relationship for linearly elastic incompressible materials [21], [32]. The additional term involving g represents the effect of growth which we assume to be isotropic (c.f. the analogous equation for isotropic thermal expansion [21]). The factor $1/3$ is required for consistency with the definition of g; taking the trace of (7) yields $g = \nabla.\mathbf{u}$ which is the correct expression for the fractional volume change.

Now equation (7) applies provided that the change in g is sufficiently small and that $\mathbf{u}$ and $\boldsymbol{\sigma}$ represent infinitesimal changes in a quasi-stationary medium. In our case, however, there is continuous volume production which creates movement and, over a period of time, finite displacement. Thus, while equation (7) may represent the principles of the relationship, it is not in a form immediately applicable to our problem. To obtain such a form we differentiate equation (7) with respect to time, using a total derivative since we are considering changes within a material element and, therefore, must follow the element. The derivative must also be objective since it is a general principle that constitutive laws be invariant if re-formulated in an arbitrarily rotating frame [3]. Invariance can be achieved in several ways but the most natural here is to take a corotational or Jaumann derivative which follows a material element with a frame that rotates with the local angular velocity. The Jaumann derivative of the strain tensor is the rate of strain tensor (see, for example, [3] for a proof) and the derivative of the growth term g produces the *rate* of volume growth per unit volume. This term can be identified with either its physical cause ($\alpha c - k$) or, more directly, from its definition, with $\nabla.\mathbf{v}$. The two terms are equal, of course, by equation (4). Combining these ideas we deduce that the appropriate constitutive law to describe a linearly elastic tumour, subject to continuous volume growth, is as follows

$$\frac{1}{2}\left(\nabla\mathbf{v} + \nabla\mathbf{v}^T\right) = \frac{1}{3}(\nabla.\mathbf{v})\boldsymbol{\delta} + \frac{1}{2E}\left\{\frac{D}{Dt}(3\boldsymbol{\sigma} - Tr(\boldsymbol{\sigma})\boldsymbol{\delta}) + 3(\boldsymbol{\omega}.\boldsymbol{\sigma} - \boldsymbol{\sigma}.\boldsymbol{\omega})\right\}, \tag{8}$$

where $\boldsymbol{\omega}$ is the second order vorticity tensor

$$\boldsymbol{\omega} = -\frac{1}{2}\left(\nabla\mathbf{v} - \nabla\mathbf{v}^T\right). \tag{9}$$

We remark that a similar constitutive law is presented in [29] to describe swelling in poroelastic media.

In the remainder of this paper we only consider situations for which $\boldsymbol{\omega} = 0$. Note that we have assumed that Young's modulus, E, is a constant. In physical terms, this implies that a change in stress always produces the same proportionate change in strain, regardless of the degree of strain. This is probably a reasonable approximation for small and even medium deformations of the tumour, but is likely to be less reliable for large deformations. Nor does it contain any consideration of the way in which growth and death processes (which are internal, microscopic processes on the scale that we are viewing the problem) may affect the elastic response.

To summarise, our model comprises equations (3)–(6), (8), (9). These define the evolution of $c, \boldsymbol{v}, \Gamma$ and $\boldsymbol{\sigma}$. In practice, boundary and initial conditions must

be imposed to close the model. Since in the following sections of the paper the model equations are solved for three different situations which warrant different boundary and initial conditions, their prescription will be considered for each case in turn. In the first case, tumour growth is assumed to take place within a semi-infinite rectangular tube so that growth is one-dimensional, occurring parallel to the axis of the tube. This situation is only realised when there is no cell death within the tumour and is, therefore, not physically realistic. However, the simple solution structure provides valuable insight into the way in which stress is produced by cell growth. In the second case the rectangular geometry and one-dimensional growth are maintained but we assume that the tumour occupies a finite section of the tube. This enables us to re-introduce cell death and to study its effect within a simple geometric configuration. Finally, we consider the more realistic case of a spherical tumour growing with radial symmetry.

Before studying the different situations described above, it is convenient to re-cast our mathematical model in dimensionless form, and thereby to identify the key dimensionless parameter groupings. This is achieved by rescaling distance with the nutrient diffusion length scale $L = \sqrt{D_c/m}$, time with the tumour doubling time $T = 1/\alpha C_0$, and the nutrient concentration with its externally-supplied value C_0 (which is assumed fixed). Denoting dimensionless quantities by tildes, we write

$$\tilde{\boldsymbol{r}} = \boldsymbol{r}/L, \qquad \tilde{t} = t/T, \qquad \tilde{c} = c/C_0, \qquad \tilde{\boldsymbol{v}} = \boldsymbol{v}T/L,$$

$$\tilde{\boldsymbol{\sigma}} = \boldsymbol{\sigma}/E, \qquad \tilde{\boldsymbol{\omega}} = \boldsymbol{\omega}T \ .$$

Under this transformation the model equations become (dropping the tildes for clarity)

$$0 = \nabla^2 c - c \ , \tag{10}$$

$$\nabla.\mathbf{v} = c - \epsilon, \tag{11}$$

$$\frac{\partial \Gamma}{\partial t} + (\mathbf{v}.\nabla)\Gamma = 0 \quad \text{on} \quad \Gamma = 0 \ , \tag{12}$$

$$\nabla.\boldsymbol{\sigma} = \mathbf{0}, \tag{13}$$

$$\frac{1}{2}\left(\nabla\mathbf{v} + \nabla\mathbf{v}^T\right) = \frac{1}{3}(\nabla.\mathbf{v})\boldsymbol{\delta} + \frac{1}{2}\left\{\frac{D}{Dt}(3\boldsymbol{\sigma} - Tr(\boldsymbol{\sigma})\boldsymbol{\delta}) + 3(\boldsymbol{\omega}.\boldsymbol{\sigma} - \boldsymbol{\sigma}.\boldsymbol{\omega})\right\}, \tag{14}$$

where

$$\boldsymbol{\omega} = -\frac{1}{2}\left(\nabla\mathbf{v} - \nabla\mathbf{v}^T\right) \tag{15}$$

and ϵ satisfies

$$\epsilon = Tk = \frac{k}{\alpha C_0}.$$

We remark that if the initial tumour size is prescribed then this gives rise to a second dimensionless parameter. For example, if in dimensional variables $r = a_0$ at $t = 0$ is prescribed then in dimensionless variables $\tilde{r} = \tilde{a_0} = a_0\sqrt{D_c/m}$. In the remainder of this paper we focus on the nondimensional equations (10)–(15).

3. 1-D tumour growth in a smooth, semi-infinite rectangular tube

In this section the model equations are formulated in terms of Cartesian coordinates (x, y, z), with x directed along the length of the tube, in the direction of growth. Writing $\Gamma(\boldsymbol{r}, t) = x - a(t)$ so that $x = a(t)$ denotes the position of the tumour surface at time t, and the tumour occupies the region $x < a(t)$. We assume that $a(0) = 0$ and that the tumour is initially in a state of zero stress. For the model to have meaning we fix $\epsilon = 0$ in equation (11). Otherwise, if cells were dying at a finite rate, however small, the infinite amount of material present would cause the tumour to collapse at infinite speed.

For the assumed geometry equation (10) takes the form

$$\frac{\partial^2 c}{\partial x^2} = c. \tag{16}$$

We solve equation (16) subject to the boundary conditions

$$c(a(t), t) = 1 \text{ and } \frac{\partial c}{\partial x} \to 0 \text{ as } x \to -\infty,$$

the latter condition ensuring that the solutions are bounded. In this way we find

$$c(x, t) = \mathrm{e}^{x-a(t)}. \tag{17}$$

With $\epsilon = 0$ equation (11) reduces to

$$\frac{\partial v}{\partial x} = c. \tag{18}$$

Again, to ensure bounded solutions, we solve equation (18) subject to the condition

$$v(x, t) \to 0 \quad \text{as} \quad x \to -\infty,$$

and deduce that

$$v(x, t) = e^{x-a}. \tag{19}$$

Using equation (12) we note that on the tumour surface

$$\frac{da}{dt} = v(a(t), t) = 1, \quad \text{with } a(0) = 0. \tag{20}$$

Thus

$$a = t, \tag{21}$$

that is, the tumour grows linearly with time.

Exploiting the geometry of the problem, we assume that the off-diagonal elements of the stress tensor, σ_{xy}, σ_{yz} and σ_{zx}, are all zero. Denoting by σ_x, σ_y and σ_z the diagonal elements, the component of (12) in the x-direction leads to the equation

$$\frac{\partial \sigma_x}{\partial x} = 0. \tag{22}$$

Assuming that there is no normal stress at the tumour boundary and scaling pressure so that the pressure outside the tumour is zero, we integrate (22) subject to the boundary condition $\sigma_x = 0$ at $x = a(t)$ in which case

$$\sigma_x = 0 \quad \forall\, x, t. \tag{23}$$

Resolution of (12) in the y- and z-directions leads to ordinary differential equations for σ_y and σ_z which are similar in form to (22) and can be integrated to show the more limited results

$$\sigma_y = \sigma_y(x, z; t) \quad \text{and} \quad \sigma_z = \sigma_z(x, y; t). \tag{24}$$

Finally we turn to the constitutive law, equation (14). When expressed in Cartesian coordinates this takes the form

$$\frac{1}{3}\frac{\partial v}{\partial x}\begin{pmatrix} 2 & 0 & 0 \\ 0 & -1 & 0 \\ 0 & 0 & -1 \end{pmatrix} = \frac{1}{2}\left(\frac{\partial}{\partial t} + v\frac{\partial}{\partial x}\right)\begin{pmatrix} -\sigma_y - \sigma_z & 0 & 0 \\ 0 & 2\sigma_y - \sigma_z & 0 \\ 0 & 0 & 2\sigma_z - \sigma_y \end{pmatrix}. \tag{25}$$

Thus only three non-trivial equations arise, of which only two are linearly independent since the trace of the system necessarily reduces to zero. The linearly independent equations may be combined to yield more convenient forms. For example, subtraction of the zz- from the yy-equation leads to

$$\left(\frac{\partial}{\partial t} + v\frac{\partial}{\partial x}\right)(\sigma_y - \sigma_z) = 0. \tag{26}$$

Imposing the boundary conditions that σ_y and σ_z both approach zero as $x \to -\infty$ and recalling that $\sigma_y = \sigma_z = 0$ at $t = 0$, we deduce that, since $v \geq 0$, $\sigma_y = \sigma_z$ throughout the tumour. Combining this result with (24) it follows that both σ_y and σ_z depend on x and t only. We introduce $\sigma(x, t)$ (no subscript) to denote this joint function, so that

$$\sigma_y \equiv \sigma_z \equiv \sigma(x, t). \tag{27}$$

Substituting (27) into any of equations (25) leads to the following expression for σ

$$\left(\frac{\partial}{\partial t} + v\frac{\partial}{\partial x}\right)\sigma = -\frac{2}{3}\frac{\partial v}{\partial x}. \tag{28}$$

Since v is already known, equation (31) may be solved, subject to the initial condition that $\sigma = 0$ at $t = 0$, giving

$$\sigma(x, t) = -\frac{2}{3}[x + \ln(1 + \mathrm{e}^{-x} - \mathrm{e}^{-t})]. \tag{29}$$

We now discuss the significance of our results. From (17) we see that the nutrient is effectively confined to a layer of length scale $1/m$ near the surface of the tumour. Consequently, growth is concentrated near the tumour surface. Since new cells are unable to move backwards down the tube, this creates a monotonically increasing velocity profile near the surface. The total growth over the tumour surface is the same at all times, so the surface itself advances with a constant velocity V.

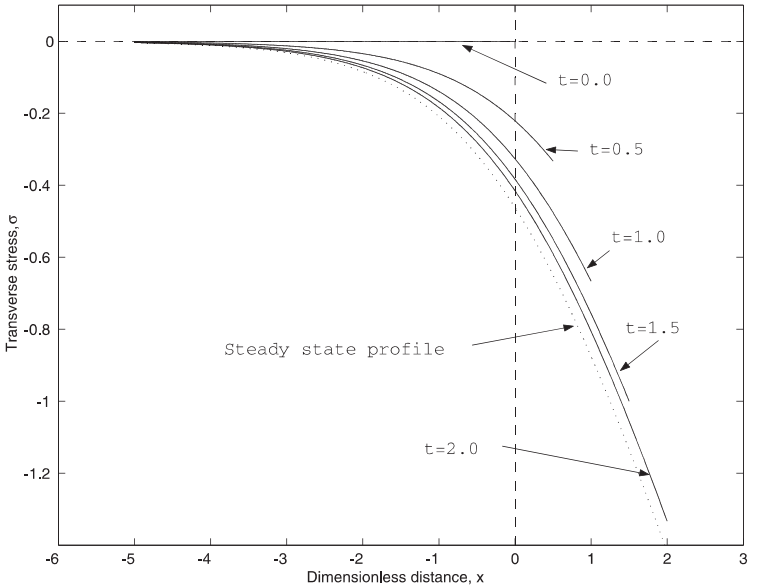

Fig. 1. Here we show how the transverse component of the stress tensor evolves within a tumour which is growing in a smooth, semi-infinite rectangular tube. Also depicted is the transverse stress profile that corresponds to the steady state tumour and to which the dynamic profiles evolve. Initially the tumour is stress-free. However, since the tube boundary prevents lateral motion of the cells, proliferation near the tumour surface generates compressive lateral stresses there. In the absence of cell death, stresses away from the tumour surface remain fixed at the values they had when the surface passed through those points. We plot $\sigma_y = \sigma_z = \sigma(x,t)$ at times $t = 0, 0.5, 1.0, 1.5, 2.0$. Key: analytical results for growing tumour (solid line); analytical results for steady state tumour (dotted line). Parameter value: $\epsilon = 0$.

Since growth is taking place in a frictionless tube, it can be accommodated without forces parallel to the tube length, and so stress components such as σ_x and τ_{yx} are zero. However, the growth is isotropic and the tumour material attempts to expand in directions perpendicular to the tube, as well as along it. The tube boundary prevents lateral motion, and so the growth generates lateral stress components, $\sigma_y = \sigma_z = \sigma(x,t)$ instead.

From the above description of the mechanism that generates the transverse stress components one would expect the long term growth pattern to exhibit the following features: (i) stresses near the surface grow linearly with time; and, (ii) the stresses in new cells not near the tumour surface are frozen at the value of the stresses in the surface that prevailed when the surface passed through that point. Since the surface moves with constant speed, this implies that the stress should increase linearly with distance away from $x = 0$. In Fig.1 we confirm these ideas by using equation (29) to plot the profiles of σ within the expanding tumour at different times. The time range in Fig.1 is relatively short ($t \sim O(1)$); the growth layer is O(1)in the figure and the new growth has only progressed a distance of

2 dimensionless units down the tube. Nevertheless the approach to a steady state profile that is linear for large x can clearly be seen in the figure. The steady state profile can be determined by letting $t \to \infty$ in equation (29) when one obtains

$$\sigma \simeq -\frac{2}{3}[x + \ln(1 + \mathrm{e}^{-x})], \tag{30}$$

and this is the dotted curve in Fig.1. It has the expected behaviour of satisfying

$$\sigma \to 0 \text{ as } x \to -\infty \text{ and } \sigma \simeq -\frac{2}{3}x \text{ for } 1 \ll x < a. \tag{31}$$

Alternatively, if we change to a moving frame of coordinates by setting $x = t + s$, so that $s = 0$ denotes the surface and the tumour occupies the region $s < 0$, then the asymptotic form for (29) as $t \to \infty$ is given by

$$\sigma \simeq -\frac{2}{3}t + s. \tag{32}$$

Equation (32) clearly shows that the stress grows linearly with time at the surface. Note that this component is negative which corresponds to the force being compressive. This is what we would expect intuitively; since lateral expansion is not permitted, the continuous lateral growth of the tumour is balanced by a transverse 'pressure'.

4. 1-D tumour growth in a bounded rectangular tube

The problem treated in this section differs from the previous problem in two respects, one minor and one major. The minor change is that the tumour is now finite in extent. We assume that initially it occupies the region $0 < x < a_0$, and that $x = 0$ is a rigid impermeable boundary so that expansion is only possible in the positive x-direction. The major difference is that we now reintroduce cell death into our model since, with only a finite amount of material present, this produces no logical inconsistencies. Thus in equation (11) we take $\epsilon > 0$.

By following a similar approach to that employed in section 3, it is possible to derive analytical expressions for the nutrient concentration, the cell velocity and the tumour growth rate. The boundary and initial conditions that we impose are the same as those used in section 3, the only difference being that those boundary conditions that were imposed at $x = -\infty$ in section 3 are now imposed at $x = 0$. Summarising these results, we have

$$c(x, t) = \frac{\cosh x}{\cosh a}, \tag{33}$$

$$v(x, t) = \left(\frac{\sinh x}{\cosh a} - \epsilon x\right) \tag{34}$$

and

$$\frac{da}{dt} = v(a, t) = \tanh a - \epsilon a. \tag{35}$$

Equation (35) has no convenient closed form integral. The force balance and constitutive law lead to results that are similar to those stated in section 3, the principal ones being that

$$\sigma_x = 0 \text{ and } \sigma_y = \sigma_z = \sigma(x,t) \ . \tag{36}$$

The partial differential equation governing σ is similar to equation (28). After substitution for $\partial v/\partial x$, the equation for σ takes the form

$$\frac{D\sigma}{Dt} = \left(\frac{\partial}{\partial t} + v\frac{\partial}{\partial x}\right)\sigma = -\frac{2}{3}\left(\frac{\cosh x}{\cosh a} - \epsilon\right) \ . \tag{37}$$

We now interpret our results and compare them with the results for the infinite tube. First note that the solution is trivial if $\epsilon > 1$. Since death everywhere exceeds growth and the tumour shrinks to nonexistence. This behaviour can be seen clearly in (35) where the right hand side is always negative if $\epsilon > 1$: as $a \to 0$ equation (35) has the approximate solution $a \simeq A\mathrm{e}^{-(\epsilon-1)t}$, where A is a constant.

Henceforth we shall consider only $\epsilon < 1$. It is easy to verify that in this case the solution of (35) always approaches a positive constant value a^* as $t \to \infty$, where a^* is the positive root of the equation

$$\frac{\tanh(a^*)}{a^*} = \epsilon \ . \tag{38}$$

This occurs irrespective of whether a is initially above or below a^* [6], [7], [12], [20]. Thus, unlike the previous case, the tumour does not grow indefinitely but eventually equilibrates at a finite size where the overall growth and death processes are in balance.

While an equilibrium is always reached, we can distinguish two physically distinct forms that the equilibrium can take. The first distinguished form occurs when ϵ is close to unity and equation (38) has the approximate solution $a^* = \sqrt{3(1-\epsilon)}$. Now, as can be seen from (33), $L = \sqrt{D_c/m}$ is the dimensional length scale over which the nutrient is able to diffuse into the tumour from the free surface. In this case the tumour is small in comparison to the diffusive length scale and this allows us to approximate (33) to $c = 1$. Hence, the nutrient concentration is approximately uniform, and death and growth processes are in approximate balance locally at every point within the tumour. This may be contrasted with the solution where $\epsilon \ll 1$ which corresponds to a death rate far below the maximum possible growth rate. In this case (38) has the approximate solution $a^* = 1/\epsilon$, and so the tumour is large when measured on the diffusive length scale. This allows us to approximate (33) as $c = \mathrm{e}^{x-a}$, showing that the nutrient concentration is only significant in a region of physical length L near the tumour surface. The overall balance between life and death is achieved by having a large growth rate in a thin region near the tumour surface, and a low death rate throughout the tumour [7].

Henceforth we assume for three reasons that $0 < \epsilon \ll 1$. First the solution has a more resolved structure when $0 < \epsilon \ll 1$, and discussion is often simplified by the ability to physically distinguish separate growth and decay regions. Secondly, when $\epsilon = \mathrm{O}(1)$, the description can still be applied, but to a joint growth/decay region. Finally, it seems unlikely that the value of ϵ would fall within such a highly

specific range (for the spherical case, numerical simulations indicate that the two-region structure is observable for $1/\epsilon > 3$), and so we expect $\epsilon \ll 1$ to be the case that occurs most commonly.

Turning to the components of the stress tensor, we note that the rectilinear geometry still permits a solution with zero axial stress ($\sigma_x = 0$) and compressive lateral stress. Before determining the lateral stress, we interpret equation (37). The left hand side of (37) defines the rate of change of σ within any material element as it is followed in time, and the right hand side is its magnitude. To simplify the discussion, let us suppose that $a(t) = a_0 = a^*$, *i.e.* the tumour starts from its equilibrium size. Then we can neglect the transient period required to attain the equilibrium size. In addition, the rate of change of σ only depends on the position of the material element within the tumour, and not on time directly. Referring to (37), we see that the rate of change of stress is O(1) and negative (compressive) for cells near the surface $x = a^*$, but is positive (tensile) and relatively small, $\mathrm{O}(\epsilon) = \mathrm{O}(k)$ away from the surface.

To determine the stress at the point (x, t) we focus attention on the path that the material particle has taken to reach that point at that time, *i.e.* we need the particle history. This is found by integrating equation (34) which is now more conveniently expressed in the form

$$v = \frac{Dx}{Dt} = V\left(\frac{\sinh x}{\cosh a^*} - \epsilon x\right) \quad . \tag{39}$$

Since $a = a^*$, we consider only stress changes that occur in the steady state growth phase of the tumour; the stress that develops during the transient stage, as it reaches its equilibrium size, is not discussed. We are interested in understanding how the stress develops for large times. Two arguments lead to useful results. The first is based on a qualitative description of the system and provides insight into how and where the stress is generated. The second method is a technical calculation which leads to a more accurate estimate of the stress.

Recall that $\epsilon \ll 1$ and, hence, from (38), that $a^* \sim 1/\epsilon$. Thus the velocity profile has a boundary layer structure. It is zero at $x = 0$ and decreases approximately linearly with x, approaching the (asymptotic) value of -1 near the surface where $x \sim 1/\epsilon$. Then, in a region of scale $x = \mathrm{O}(1)$ it increases sharply, achieving zero at the surface.

Consider now a material particle that is in the tumour at a suitably large time. Since the velocity is everywhere and at all times negative, the particle must have travelled backwards from the direction of the surface to reach its current position. Further, its speed within the tumour bulk, and within most of the extent of the surface boundary layer, is O(1). Thus the substantial part of the distance from the surface would have been crossed in a time of $\mathrm{O}(a^*)$. If, however, $t \gg a^*$, then at $t = 0$ the particle must have been in very close proximity to the surface. At the surface the velocity field approaches zero and the time for the particle to escape can be indefinitely large, depending on the exact degree of initial proximity. Therefore a particle that is in the interior at large times will have spent most of its existence at the surface $x = a^*$, and have moved into the interior in its relatively recent past.

In this case (37) supplies $D\sigma/Dt \sim -2v/3$ so that

$$\sigma \sim -\frac{2}{3}t \ . \tag{40}$$

Since the particle spends most of its time at the surface, the positive growth rate there is dominant and the negative growth rate in the interior plays a secondary role.

With this understanding, we now use (37) to derive a more accurate estimate of σ. Let $s = (a^* - x)$ represent the distance from the tumour surface. Since $a^* \sim 1/\epsilon$, we deduce from (39) that

$$\frac{Ds}{Dt} \sim (1 - \epsilon s - e^{-s}) \ . \tag{41}$$

Let $x = (1 - v)a^*$ or, equivalently, $s \sim v/\epsilon$ denote a typical point in the interior of the tumour (so $v \in (0, 1)$). Then a cell which is at $s \sim v/\epsilon$ at time t was initially at position s_0 where

$$t \sim \int_{s_0}^{v/\epsilon} \frac{ds}{1 - \epsilon s - e^{-s}} \quad (+ \text{ exponential error}) \tag{42}$$

$$= \int_{s_0}^{v/\epsilon} \frac{ds}{1 - \epsilon s} + \int_{s_0}^{v/\epsilon} \frac{e^{-s} ds}{(1 - \epsilon s)(1 - \epsilon s - e^{-s})}$$

$$\sim \int_{s_0}^{v/\epsilon} \frac{ds}{1 - \epsilon s} + \int_{s_0}^{\infty} \frac{e^{-s} ds}{(1 - \epsilon s)(1 - \epsilon s - e^{-s})} \quad (+ \text{ exponential error})$$

$$\sim \frac{1}{\epsilon} \ln\left(\frac{1 - \epsilon s_0}{1 - v}\right) - \ln(1 - e^{-s_0}) + O(\epsilon) \ . \tag{43}$$

In the limit of $\epsilon \to 0$, a balance of terms is only possible if $s_0 \to 0$, as expected from the physical discussion earlier. This allows us to simplify further and deduce that

$$\ln(1 - \mathrm{e}^{-s_0}) \sim \frac{1}{\epsilon} \ln\left(\frac{1}{1 - v}\right) - t \ . \tag{44}$$

We now determine how the stress changes as the characteristic path connecting $(s_0, 0)$ to $(v/\epsilon, t)$ is traversed. Integrating (28), and expressing the result in terms of s, we obtain

$$\sigma(v/\epsilon, t) = -\frac{2}{3}\Big[\ln v\Big]_{(s_0,0)}^{(v/\epsilon,t)} \ .$$

The right-hand side of this expression is evaluated by using (41) to determine the velocity, and (44) to express s_0 in terms of t. In the limit of $s_0 \to \infty$, we re-express σ in terms of x to deduce that

$$\sigma(x, t) \sim \frac{2}{3} \ln\left(\frac{1 - \mathrm{e}^{-s_0}}{1 - v}\right) \sim -\frac{2}{3}\left[t - \left(\frac{1}{\epsilon} - 1\right) \ln\left(\frac{a^*}{x}\right)\right] \ . \tag{45}$$

Not only is this result consistent with equation (40) but it also predicts the principal spatial distribution of the stress.

The above expressions apply only for material that has been convected from the tumour surface to the interior. The deepest penetration is achieved by cells which began at the interior edge of the surface boundary layer, and for which (39) takes the asymptotic form

$$\frac{Dx_p}{Dt} \sim -\epsilon x_p, \quad x_p(0) \sim a^* \ ,$$

where $x_p(t)$ is the position reached by this particular material. This has the solution

$$x_p(t) = a^* \mathrm{e}^{-\epsilon t} \ .$$

Since this is the maximum penetration depth, it follows that all of the above asymptotic expressions, and in particular (45), only apply for $x_p(t) < x < a^*$. For material that was not generated at the surface and which currently occupies the complementary region $0 \leq x < x_p(t)$, the asymptotic form of (37) is much simpler, namely

$$\frac{D\sigma}{Dt} \sim \frac{2}{3}\epsilon \ ,$$

showing that in this region

$$\sigma(t) \sim \frac{2}{3}\epsilon t \ .$$

Physically this is easy to understand. The natural effect of cell death in the interior is to make the tumour material shrink, and so draw away from the boundary walls. However, such transverse movement is not permitted. Instead a transverse tensile force (positive σ) is generated that prevents such shrinkage.

The asymptotic curves are plotted in Fig.2 for $\epsilon = 0.1$ at various times. The change from compressive stress at the free boundary to tensile stress in the far interior is clearly discernible.

Finally, we remark that if $\epsilon > 1$, so that the tumour shrinks indefinitely, then $D\sigma/Dt > 0$. This means that the ever-decreasing amount of tumour remaining at any time experiences increasing stress. Of course, in this case the continuum model eventually fails.

5. Growth of a radially-symmetric tumour

In this section we consider the more realistic, three dimensional case of the growth of a radially symmetric spherical tumour. Although growth is no longer confined to one direction there are analogies between this case and that of growth in a finite rectangular tube. Indeed, the method of solution parallels that adopted in section 4.

In spherical polar coordinates and assuming spherical symmetry, we integrate equations (10) and (11) subject to the boundary conditions

$$v = 0 \text{ and } c \text{ is finite at } r = 0, \quad \text{and} \quad c = 1 \text{ on } r = a \ ,$$

to obtain

$$c(r,t) = \frac{a \sinh r}{r \sinh a} \ , \tag{46}$$

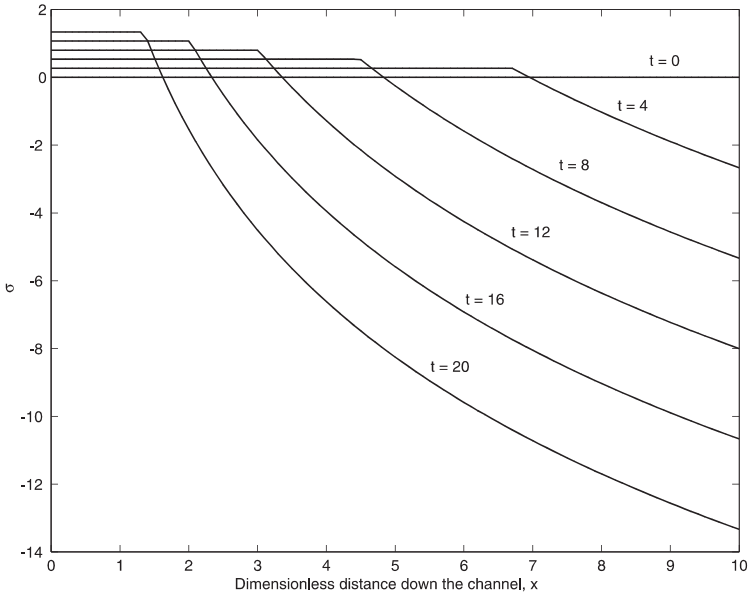

Fig. 2. Here we illustrate the asymptotic estimate of the transverse component of the stress tensor within a tumour which is in a smooth, finite rectangular tube and which began at its equilibrium size $a_0 = a^* \sim 1/\epsilon$. As in Fig. 1, cells near the tumour boundary are subject to a compressive stress ($\sigma < 0$) whose magnitude increases linearly with time. However cells near the tumour centre, where cell death dominates proliferation, are subject to a transverse tensile force ($\sigma > 0$) which also increases linearly in time. We plot σ at times $t = 0, 4, 8, \ldots, 20$. Parameter values: $\epsilon = 0.1$, $a^* \sim 1/\epsilon = 10$.

and

$$v(r,t) = \frac{a}{r^2 \sinh a}\,(r\cosh r - \sinh r) - \frac{\epsilon r}{3} \quad . \tag{47}$$

Evaluating the velocity on the tumour boundary enables us to determine the rate of growth of the tumour radius a

$$\frac{da}{dt} = v(a,t) = \coth a - \frac{1}{a} - \frac{\epsilon a}{3} \quad . \tag{48}$$

Expressed in spherical polar coordinates the force balance equation (13) becomes

$$\nabla.\boldsymbol{\sigma} = \begin{pmatrix} \dfrac{\partial \sigma_r}{\partial r} + \dfrac{1}{r}(2\sigma_r - \sigma_\theta - \sigma_\phi) \\ \dfrac{1}{r}\dfrac{\partial \sigma_\theta}{\partial \theta} + \dfrac{\cot\theta}{r}(\sigma_\theta - \sigma_\phi) \\ \dfrac{1}{\sin\theta}\dfrac{\partial \sigma_\phi}{\partial \phi} \end{pmatrix} = \mathbf{0} \quad . \tag{49}$$

In (49) we have exploited the spherical symmetry by setting the off-axis elements of the stress tensor to zero. Applying this assumption to equation (14) we deduce further that

$$\begin{pmatrix} \frac{\partial v}{\partial r} & 0 & \\ 0 & v/r & 0 \\ 0 & 0 & \frac{\partial v}{\partial r} \end{pmatrix} = \frac{1}{3r^2}\frac{\partial}{\partial r}(r^2 v)\begin{pmatrix} 1 & 0 & 0 \\ 0 & 1 & 0 \\ 0 & 0 & 1 \end{pmatrix}$$

$$+\frac{1}{2}\left(\frac{\partial}{\partial t} + v\frac{\partial}{\partial r}\right)\begin{pmatrix} 2\sigma_r - \sigma_\theta - \sigma_\phi & 0 & 0 \\ 0 & 2\sigma_\theta - \sigma_r - \sigma_\phi & 0 \\ 0 & 0 & 2\sigma_\phi - \sigma_r - \sigma_\theta \end{pmatrix} \tag{50}$$

As in section 4, the components of equation (50) contain only two independent pieces of information, and the equations must be suitably combined before they can applied. One useful equation is obtained by subtracting the $\theta\theta$- from the $\phi\phi$-equation, and can be written

$$\left(\frac{\partial}{\partial t} + v\frac{\partial}{\partial r}\right)(\sigma_\theta - \sigma_\phi) = 0.$$

Integrating this equation subject to an initial condition of zero stress (no boundary condition is needed), we deduce that $\sigma_\theta = \sigma_\phi$. Using this result we obtain a second linearly independent equation from (50) in the form

$$\left(\frac{\partial}{\partial t} + v\frac{\partial}{\partial r}\right)\beta = \frac{2}{3}r\frac{\partial}{\partial r}\left(\frac{v}{r}\right) \quad , \tag{51}$$

where

$$\beta = \sigma_r - \sigma_\theta \quad . \tag{52}$$

With $\sigma_\theta = \sigma_\phi$, equations (49) supply the additional constraints that $\sigma_\theta = \sigma_\phi$ is a function of r and t only, and also the equation

$$\frac{\partial \sigma_r}{\partial r} + \frac{2\beta}{r} = 0 \quad . \tag{53}$$

Thus the natural method of solution is first to solve (51) for β, then to solve (53) for σ_r, and finally to use (52) to determine σ_θ.

We construct model solutions in two different ways. Firstly we develop an asymptotic solution that predicts the stress for large times for tumours that are initially stress free and at their equilibrium size. In section 5.2 numerical results obtained for the full model are presented (details of the numerical method are presented in the appendix). These allow us to investigate the effect that tumour growth has on the evolving components of the stress tensor.

5.1. Asymptotic analysis

The asymptotic analysis is similar to that presented in section 4. We assume that the tumour is at its equilibrium size so that $da/dt \equiv 0$ and $a = a^*$ where, from (48),

$$0 = \coth a^* - \frac{1}{a^*} - \frac{\epsilon a^*}{3} \quad .$$

By noting that (48) has the asymptotic solution $a^* = 3/\epsilon - 1 + O(\epsilon)$ we can express equation (47) in the form:

$$v = -\frac{Ds}{Dt} = \left(e^{-s} - \frac{\epsilon}{3}(a^* - s)\right) + O(\epsilon) \quad , \tag{54}$$

where $s = a^* - r$ denotes the distance from the tumour boundary. In (54) we have retained terms of $O(\epsilon)$ which persist over the full range of s, *i.e.* $0 < s < 3/\epsilon$. and neglected terms which have exponential multipliers, and are negligible away from the region $s = O(1)$. Thus, when we integrate (54), the result has an $O(\epsilon)$ error estimate.

Equation (54) is now used to find the starting location $s = s_0$ of a material particle which at time t has location $r = a^*(1 - v)$. We do this by integrating (54) along the characteristic path connecting $(s, t) = (s_0, 0)$ and $(s, t) = (va^*, t)$, and deduce that

$$\begin{aligned} t &\sim \int_{s_0}^{va^*} \frac{ds}{\epsilon(a^* - s)/3 - \mathrm{e}^{-s}} \\ &= \frac{3}{\epsilon}\int_{s_0}^{va^*} \frac{ds}{a^* - s} + \frac{3}{\epsilon}\int_{s_0}^{va^*} \frac{\mathrm{e}^{-s} ds}{(a^* - s)(\epsilon(a^* - s)/3 - \mathrm{e}^{-s})} \\ &\sim \frac{3}{\epsilon}\ln\left(\frac{a^* - s_0}{a^* - v^* a}\right) - \int_{s_0}^{\infty} \frac{\mathrm{e}^{-s} ds}{1 - \mathrm{e}^{-s}} \\ &\sim \frac{3}{\epsilon}\ln\frac{1}{1 - v} - \ln(1 - \mathrm{e}^{-s_0}) + O(\epsilon) \quad , \end{aligned} \tag{55}$$

where the last result has been simplified by the fact that $s_0 = O(\mathrm{e}^{-1/\epsilon})$ to be significant in the overall equation.

The stress difference β is determined by integrating (51), along the same characteristic curve:

$$\beta = \frac{2}{3}\left[\ln\left(\frac{v}{r}\right)\right]_{(s_0,0)}^{(va^*,t)} \quad ,$$

where the integration limits are quoted for (s, t). We may use (54) to provide a suitable expression for v. Then, after substitution of the limits, and recalling that $s_0 = O(e^{-1/\epsilon})$, we find that

$$\begin{aligned} \beta(r, t) &\sim -\frac{2}{3}\ln(1 - \mathrm{e}^{-s_0}) \sim \frac{2}{3}\left[t + \frac{3}{\epsilon}\ln(1 - v)\right] \\ &\sim \frac{2}{3}\left[t - \frac{3}{\epsilon}\ln\left(\frac{a^*}{r}\right)\right] \quad , \end{aligned} \tag{56}$$

where s_0 has been eliminated using (55), and the final result has been rewritten in terms of r. Substituting for β in equation (53) and integrating with respect to r leads to the following expression for σ_r,

$$\sigma_r(r,t) \sim \frac{2}{3}\left[2t\ln\left(\frac{a^*}{r}\right) - \frac{3}{\epsilon}\ln^2\left(\frac{a^*}{r}\right)\right] \quad . \tag{57}$$

Finally, combining (56) and (57) with equation (52) leads to the following expression for $\sigma_\theta (= \sigma_\phi)$

$$\sigma_\theta \sim \frac{2}{3}\left\{t\left[2\ln\left(\frac{a^*}{r}\right) - 1\right] + \frac{3}{\epsilon}\ln\left(\frac{a^*}{r}\right)\left[1 - \ln\left(\frac{a^*}{r}\right)\right]\right\} \quad . \tag{58}$$

The above expressions are valid for cells that originated in the surface layer and moved into the tumour interior. The deepest penetration is achieved by cells that started at the inner edge of the layer for which equation (47) takes the asymptotic form

$$\frac{dr_p}{dt} \sim -\frac{\epsilon}{3}r_p, \quad r_p(0) \sim a^* \Rightarrow r_p = a^* \mathrm{e}^{-\epsilon t/3} \ ,$$

where r_p is the position reached by this particular material. The asymptotic solutions are applicable when $r_p(t) < r < a^*$, and are least accurate for r close to $r_p(t)$ (since then the corresponding values of s_0 are not small, contrary to the assumption in the derivation). Outside this region, the stresses take constant values such that the overall stress curve is continuous.

These results are illustrated in Figs. 3–5 where they are also compared with the numerical results. Their physical interpretation is as follows. The tumour undergoes strong growth in all directions within the surface layer. The growth in the transverse direction (tangential to the surface) has no way of accommodating this expansion by movement, and so the growth causes an increase in the stress. This increase is compressive ($\sigma_\theta < 0$), and grows linearly with time. Growth in the radial direction can be compensated by movement, however, so the radial stress remains close to zero (exactly zero on the surface itself). The death of cells within the tumour slowly draws material away from the surface layer in such a way that the stress *difference* is carried with the material (since, in the interior, $v \sim -\epsilon/3$, and so the right hand side of (51) reduces to zero). Once it leaves the boundary layer, the value of $\beta = \sigma_r - \sigma_\theta$ remains the same thereafter. While cell death in principle relieves the stresses, it also causes material to collapse inward in a manner which exactly compensates for, and maintains, the stress difference. Over time, this process creates a natural stress distribution since material drawn in at later times is in a more highly stressed state than material that entered earlier. The development of β is illustrated in Fig. 3.

While β remains the same for any piece of material, the stresses themselves do not. As indicated by (53), to draw an annular ring of material inward when the stress difference is positive requires a net tensile force in the radial direction. This is most easily appreciated for the ring of material moving in from the surface layer. This is under transverse compression with no radial stress. Clearly a tensile force (an increase in σ_r) is required to draw this inward: the natural effect of such

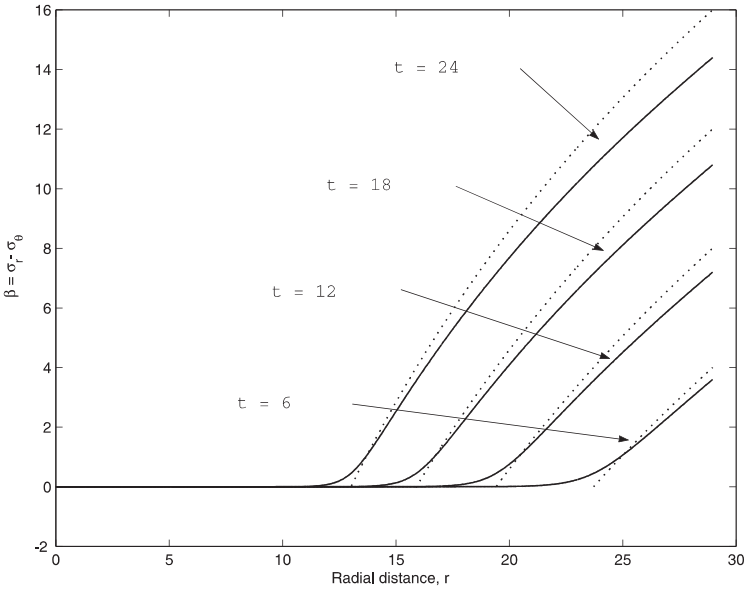

Fig. 3. Here we show how the stress difference $\beta = \sigma_r - \sigma_\theta$ evolves within an equilibrium size spherical tumour with radial symmetry. Cell death draws cells away from its surface in such a way that once it leaves the proliferating rim a cell's value of β remains fixed thereafter. Good agreement between the asymptotic solutions and the numerically constructed solutions is observed. We plot β at times $t = 0, 6, 12, 18, 24$. Key: numerical results (solid line); asymptotic profiles (dotted line). Parameter values: $\epsilon = 0.1$, $a_0 = a^* \sim 28$.

a change would be to compress the material further. This argument is true for *all* material rings that have been brought in from the surface, and so there is a net cumulative effect on the radial stress. It thus increases (becomes tensile) as one moves away from the surface towards the tumour centre. This process continues until one reaches the tumour core, *i.e.* cells that were initially present in the tumour and not generated at the surface. This material will have retained its initial value of $\beta = 0$. The radial stress σ_r thus ceases to change in this region (see (53)), and adopts a uniform, positive value. Notice that although σ_r is spatially uniform in the core, its value increases with time. Physically, a low 'pressure' is required in the core to draw pre-stressed material inward from the surface. Technically the value of σ_r equals the integral of $2\beta/r$ over the whole exterior region and the values of β in the region exterior to the core are increasing. This increase occurs in two ways: β is increasing linearly with time at the surface, and the extent of the exterior region is itself growing with time as the core shrinks. At early times the combination of these two effects causes the rate of increase of σ_r to be positive also. This early acceleration of growth can be seen in Fig. 4, although at large times the core shrinks and the effect becomes less marked.

Finally, since σ_r is positive in the core, and the stress difference there is identically zero,it follows that the transverse stress σ_θ is also positive everywhere in the

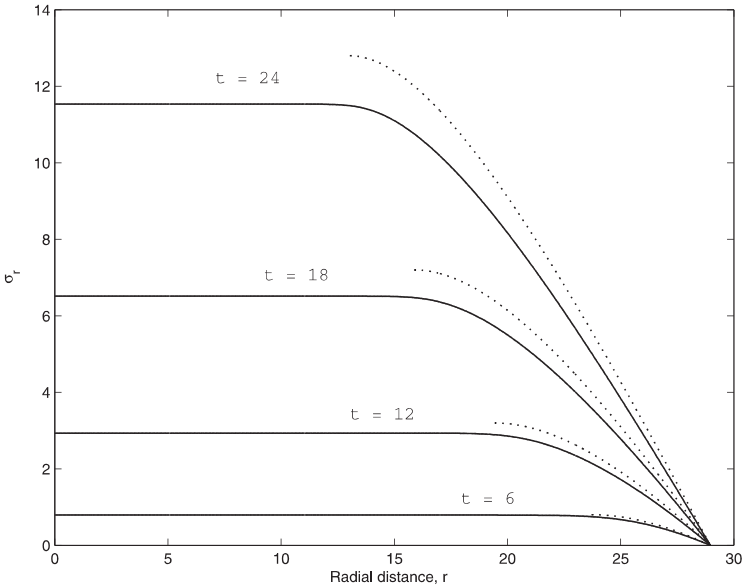

Fig. 4. Here we show how $\sigma_r(r, t)$ develops within an equilibrium size spherical tumour with radial symmetry. A tensile stress ($\sigma_r > 0$) which increases over time develops as cells are drawn towards the centre of the tumour. We plot σ_r at times $t = 0, 6, 12, 18, 24$. Key and parameter values: as per Fig. 3.

core region. Thus, although the transverse stress is initially compressive near the surface, it must eventually become tensile as it approaches the centre. This can be seen in Fig. 5.

If we compare the stress development for the spherical tumour with that for the finite rectangular tube we see that the difference in geometry causes significant differences. Whilst in both cases the stresses are generated by strong growth at the surface they are modified in different ways as material is drawn into the interior by the slow death rate. For the rectangular tube, motion normal to the free surface, *i.e.* parallel to the tube, is achievable with no axial stress component. For the sphere the corresponding flow is radial, and the convergence of this flow requires a positive stress gradient (so the radial stress reduces and becomes tensile towards the sphere centre). For the rectangular tube, shrinkage in the transverse direction cannot be accommodated by any lateral motion. Instead, there has to be a stress change which must be positive (σ goes from being a negative compression near the surface to a positive tension in the interior). This also contrasts with the sphere where the movement of a ring of material towards the centre does help compensate for 'lateral', *i.e.* azimuthal, shrinkage. However, the compensation is only exactly balanced for unstressed material. For the pre-stressed material generated at the surface there is a net change in the azimuthal stress. In fact the stress *difference*, $\beta = \sigma_r - \sigma_\theta$, remains the same as material is convected towardsthe centre, so

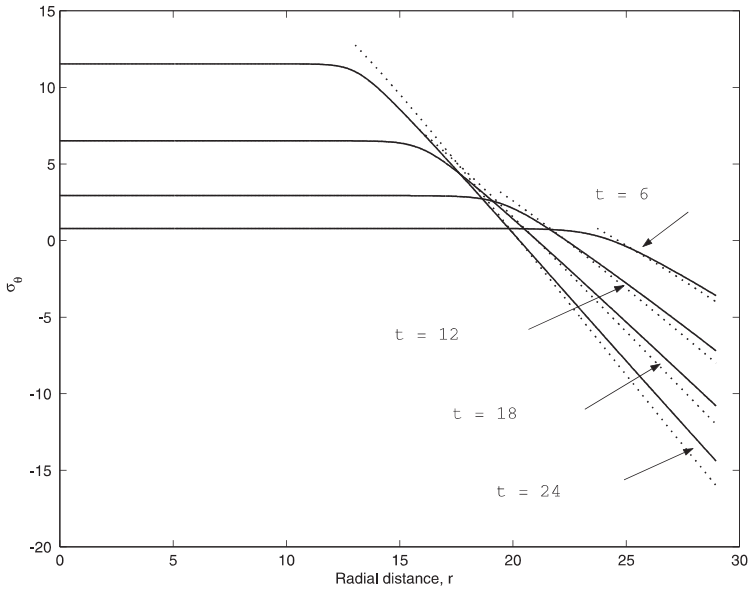

Fig. 5. Here we show how $\sigma_\theta(r, t)$ develops within an equilibrium size spherical tumour with radial symmetry. The profiles are qualitatively similar to those presented in Fig. 2. We plot σ_θ at times $t = 0, 6, 12, 18, 24$. Key and parameter values: as per Fig. 3.

the fact that the radial stress is increasing means that the azimuthal stress must increase also.

5.2. Numerical results

The asymptotic results described above apply to steady state situation where the tumour is initially stress free, and at its equilibrium size $a = a^*$. To investigate more general situations we obtain solutions by numerical means. The numerical procedure has four distinct stages. Firstly a simple numerical integration is performed on (48) to determine a at the next time stage. With a known, (47) is used to calculate v everywhere within the tumour. Secondly an extension of the Lax-Wendroff integration scheme is used to solve the hyperbolic equation (51) for β. The extension is needed to account for the fact that the integration domain is time dependent (further details are included in the appendix). Thirdly (53) is used to determine σ_r via a simple numerical integration, and finally σ_θ follows from (52) by subtraction.

As a first application of the computer program we verified the asymptotic formulae derived earlier by plotting them on the same graphs as the asymptotic results. The numerical results are the solid curves in Figs. 3–5, and the asymptotic results are the dotted curves. The estimated error in the asymptotic formulae is $O(\epsilon)$; the value of ϵ is 0.1 for these curves, and it can be seen that the asymptotic predictions fall within 10% of the numerical calculations.

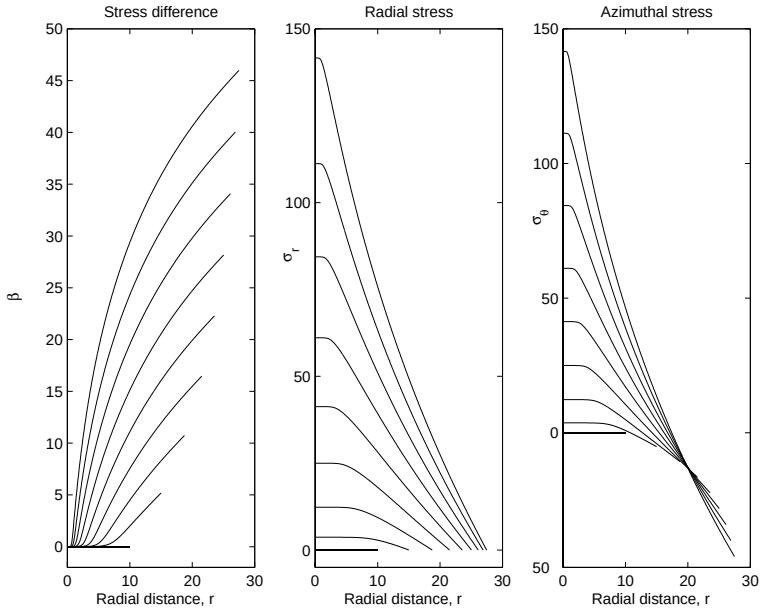

Fig. 6. Here we show how $\beta = \sigma_r - \sigma_\theta$, σ_r and σ_θ evolve within a radially-symmetric spherical tumour which is growing. As in Figs. 3–5, a compressive azimuthal stress develops near the surface of the tumour whereas cell death near the centre leads to increases in both σ_r and σ_θ over time. Since the proportion of cells initially present in the tumour decreases more rapidly for the growing tumour depicted here than for the equilibrium tumour of Figs. 3–5, the plateau region where σ_r and σ_θ attain constant values decreases more rapidly than in Figs. 3–5. We plot β, σ_r and σ_θ at times $t = 0, 10, 20, \ldots, 80$ for a tumour of initial size about a third of its equilibrium size. Parameter values: $a_0 = 10, \epsilon = 0.1$.

Numerical results for a growing tumour are illustrated in Fig. 6. As before we fix $\epsilon = 0.1$ and assume that the tumour is initially stress free, with size $a = 10$. Plots of β, σ_r and σ_θ at equal time increments are presented in Fig. 6 and over this period the tumour effectively reaches its equilibrium size of $a^* \sim 28.96$.

The features described in section 5.1 for the equilibrium size tumour can be seen here also, namely that compressive azimuthal stress is generated principally at the surface, the radial/azimuthal stress difference is convected unchanged into the interior, and cell death creates an increase in both the radial and azimuthal stress as this convection proceeds. The major difference between this case and the equilibrium case is in the relative extent of material originally present in the tumour, *i.e.* material not produced by surface growth. This material is easily identified as the region in which β remains equal to zero. For the equilibrium tumour, this material occupies most of the tumour initially. As this material dies, new material is drawn in to replace it, but to replace such a large amount of material takes time. By contrast, in the time dependent case, the initial material occupies a much smaller fraction of the eventual tumour volume. New, stressed, material is actually created 'inside' the tumour as the growing-surface traverses locations that eventually become interior points. Consequently, the visual impact of the region of original material is

diminished in the time dependent case, although the physical mechanism driving the stress changes is the same.

6. Conclusions

In this paper we have developed a mathematical model of avascular tumour growth. It describes the effect of differential growth on the mechanical stress experienced by the constituent cells. As such, the model represents a first attempt to describe the way in which cell proliferation, growth and death interact with mechanical properties of the tumour such as its stress and strain. Since cell proliferation and death are continuous processes that are usually defined as rates, the constitutive law that we used to describe the tumour relates the rate of change of the stress tensor to the rate of change of the strain tensor, with an additional term included to describe the manner in which changes in the changes in the cell number (the net result of proliferation, growth and death) affect the stress rate. The mathematical model that we developed was applied to three different one-dimensional geometries: growth in a smooth, semi-infinite rectangular tube, growth in a smooth, finite rectangular tube, and growth of a radially-symmetric tumour. The numerical and analytical results used to study the model revealed several common features. First, cells near the tumour boundary, where nutrient levels and cell proliferation rates are high, are under compression. By contrast, cells towards the centre of the tumour, where nutrient levels are low and cell death dominant, are under tension.

One of the main weaknesses of the model is its failure to predict the existence of a steady state profile for the stress tensor. By following [19], [26] and [27] and modelling the tumour as a multiphase medium, which contains extracellular water, live tumour cells and dead tumour cells, it may be possible to resolve this issue. In particular, in regions of the tumour where the number of live cells is low the compensatory increase in the number of dead cells and extracellular water should prevent the stress tensor increasing indefinitely over time. In addition, we will continue to model the tumour cells as a deformable elastic continuum. Experimental results which support this description were obtained by Helmlinger *et al.* [15]: they observed that the constituent cells of tumour spheroids became more densely packed as the concentration of the agarose gel in which they were growing increased, *i.e.* the cells are deformable. By introducing separate variables to describe dead cells and extracellular water it should be possible to predict the initiation and development of the necrotic core which is commonly observed in well-developed avascular tumours and multicellular spheroids.

Other features which should be addressed in future models include distinguishing between cell growth and cell division: intuitively we anticipate that, unlike cell growth or expansion, cell division will cause a relaxation in the local stress field and that this difference should be incorporated into the constitutive law. Moreover by including proliferation terms which depend upon the stress tensor we aim to investigate the effect of stress-dependent growth.

Helmlinger *et al.*'s experimental results [15], which were described above, highlight the role of interactions between the tumour cells and the media into which they are invading. By extending the modelling framework presented in this paper

to include the surrounding tissue matrix or gel it will be possible to compare the ability of different tissues, with different constitutive laws, to offer resistance to the invading tumour cells. Such analysis may provide a link between the degree of aggression of invasiveness of tumours and that of their host tissue.

As stated above, our mathematical model is a first attempt to describe the way in which mechanical effects interact with growth processes in deformable biological tissues such as tumours. (Other applications included bone, tendons and ligaments.) There are many ways in which the model could be improved and rendered more physically realistic. For example, in its present form, the impact of mechanical interactions with the external environment are neglected.

Appendix

The Lax-Wendroff method is a second order accurate finite difference scheme for hyperbolic differential equations which, as in our situation, do not develop discontinuities. For the standard scheme with a fixed grid, an expression for the dependent variable β at an advanced time level $(j+1)$, where j is a counter such that $t_j = j\delta t$, is developed in three steps:- (i) a second order Taylor series expansion for β is made about the time level $j+1$, (ii) the partial differential equation (51) is used to eliminate terms involving time derivatives of β, and (iii) finite difference approximations are applied to the spatial derivatives. In our case the spatial domain (*i.e.* the tumour) evolves over time. To accommodate this, we represent the solution at any time level by its values at a fixed *number* of points where the points are *evenly distributed* over the tumour domain. Consequently the grid consists of *moving* points, a fact which must be accounted for when developing the Lax-Wendroff integration scheme.

Let i be a spatial counter such that $r_{i,j} = i\delta r_j$, $0 \le i \le i_{\max}$, where δr_j is a function of t_j such that $i_{\max}\delta r_j = a(t_j)$. Let $u_{i,j} = v(a, t_j)i/i_{\max}$ be the speed of the ith grid point at time t_j. Then

$$\begin{aligned}\beta_{i,j+1} &= \beta\,(r+U, t+\delta t)\\ &\sim \beta(r,t) + \frac{\partial\beta}{\partial r}U + \frac{\partial\beta}{\partial t}\,\delta t\\ &\quad + \frac{1}{2}\frac{\partial^2\beta}{\partial r^2}U^2 + \frac{\partial^2\beta}{\partial r\partial t}U\delta t + \frac{1}{2}\frac{\partial^2\beta}{\partial t^2}\,\delta t^2\ ,\end{aligned} \tag{59}$$

where

$$U(t) = \int_t^{t+\delta t} u(\tau)d\tau\ ,$$

r denotes $r_{i,j}$, u denotes $u_{i,j}$, and t denotes t_j, the subscripts having been omitted to assist legibility. The time integral in (59) is expanded in powers of δt, and the equation (51) is used to eliminate all time derivatives of β. After approximating the remaining spatial derivatives as finite differences, we obtain the iteration formula

$$\beta_{i,j+1} = \beta_{i,j}\left[1 - \frac{1}{2}\left(\frac{\delta t}{\delta r}\right)^2 (u^2 - 2uv + v^2)\right]_{i,j}$$
$$+ (\beta_{i+1,j} - \beta_{i-1,j})\left[(u - v) + \frac{\delta t}{2\delta r}\left(v\frac{\partial v}{\partial r} - 2u\frac{\partial v}{\partial r} + \frac{\partial u}{\partial t} - \frac{\partial v}{\partial t}\right)\right]_{i,j}\frac{\delta t}{2\delta r}$$
$$+ (\beta_{i+1,j} + \beta_{i-1,j})\left(u^2 - 2uv + v^2\right)_{i,j}\left(\frac{\delta t}{2\delta r}\right)^2$$
$$+ \delta t\,\gamma_{i,j} + \frac{\delta t^2}{2}\left(\frac{\partial \gamma}{\partial t} + \frac{\partial \gamma}{\partial r}(2u - v)\right)_{i,j}, \qquad (60)$$

where $\gamma = (2r/3)\partial(v/r)/\partial r$, the right hand side of (51), and u denotes the value of $u_{i,j}$ as above. Notice that no boundary conditions are needed since both boundaries $r = 0$ and $r = a(t)$ are characteristics of the system.

References

1. Adam, J.A.: A mathematical model of tumour growth. II Effects of geometry and spatial uniformity on stability. Math. Biosci. **86**, 183–211 (1987)
2. Anderson, A.R.A., Chaplain, M.A.J.: Continuous and discrete mathematical models of tumour-induced angiogenesis. Bull. Math. Biol. **60**, 857–899 (1998)
3. Bird, R.B. Armstrong, R.C., Hassager, O.: Dynamics of polymeric liquids, Chapter 7, John Wiley & Sons, 1977
4. Burton, K., Taylor, D.L.: Traction forces of cytokinesis measured in optically modified elastic substrata. Nature, **385**, 450–454
5. Byrne, H.M., Chaplain, M.A.J.: Mathematical models for tumour angiogenesis: Numerical simulations and nonlinear wave solutions. Bull. Math. Biol. **57**, 461–486 (1995)
6. Byrne, H.M., Chaplain, M.A.J.: Modelling the role of cell-cell adhesion in the growth and development of carcinomas. Math. Comput. Modell. **24**, 1–17 (1996)
7. Byrne, H.M., Chaplain, M.A.J.: Necrosis and apoptosis: distinct cell loss mechanisms in a mathematical model of avascular tumour growth. J. Theor. Med. **1**, 223–235 (1998)
8. Chaplain, M.A.J., Sleeman, B.D.: Modelling the growth of solid tumours incorporating a method for their classification using non-linear elasticity theory. J. Math. Biol. **31**, 431–473 (1993)
9. Drozdov, A.D., Khanina, H.: A model for the volumetric growth of a soft tissue. Math. Comput. Modell. **25**, 11–29 (1997)
10. Folkman, H., Brem, H.: Angiogenesis and inflammation. In: Inflammation: Basic Principles and Clinical Correlates, Second Edition. (eds. Gallin, J.I., Goldstein, I.M., Snyderman, R.). New York: Raven Press (1992)
11. Folkman, J., Hochberg, M.: Self-regulation of growth in three dimensions. J. Exp. Med. **138**, 745–753 (1973)
12. Friedman, A., Reitich, F.: Analysis of a mathematical model for the growth of tumours. J. Math. Biol. **38**, 262–284 (1999)
13. Graeber, T.G., Osmanianm, C., Jacks, T., Housman, D.E., Koch, C.J., Lowe, S.W., Giaccia, A.J.: Hypoxia-mediated selection of cells with diminished apoptotic potential in solid tumours. Nature **379**, 88–91 (1996)
14. Greenspan, H.P.: Models for the growth of a solid tumour by diffusion. Stud. Appl. Math. **52**, 317–340 (1972)

15. Helmlinger, G., Netti, P.A., Lichtenbeld, H.C., Melder, R.J., Jain, R.K.: Solid stress inhibits the growth of multicellular tumour spheroids. Nature Biotech. **15**, 778–783 (1997)
16. Jackson, T.L., Senter, P.D., Murray, J.D.: Development and validation of a mathematical model to describe anti-cancer prodrug activation by antibody-enzyme conjugates, J. Theor. Med. (To appear, 1999)
17. Kerr, J.F.R.: Shrinkage necrosis; a distinct mode of cellular death. J. Path. **105**, 13–20 (1971)
18. Kerr, J.F.R., Wyllie, A.H., Currie, A.R.: Apoptosis: a basic biological phenomenon with wide-ranging implications in tissue kinetics. Br. J. Cancer **26**, 239–257 (1972)
19. Landman, K.A., Please, C.P.: Tumour dynamics and necrosis: surface tension and stability. J. Theor. Med. (submitted)
20. McElwain, D.L.S., Morris, L.E.: Apoptosis as a volume loss mechanism in mathematical models of solid tumour growth. Math. Biosci. **39**, 147–157 (1978)
21. Malvern, L.E.: Introduction to the mechanics of a continuous medium. Prentice Hall, New Jersey, 1969
22. Muthukkaruppan, V.R., Kubai, L., Auerbach, R.: Tumor-induced neovascularisation in the mouse eye. J. Natn. Cancer Inst. **69**, 699–705 (1982)
23. Orme, M.E., Chaplain, M.A.J.: Two-dimensional models of tumour angiogenesis and anti-angiogenesis strategies. IMA J. Math. Appl. Med. Biol. **14**, 189–205 (1997)
24. Paweletz, N., Knierim, M.: Tumor-related angiogenesis. Crit. Rev. Oncol. Hematol. **9**, 197–242 (1989)
25. Perumpanani, A.J., Byrne, H.M.: Extracellular matrix concentration exerts selection pressure on invasive cells, Eur. J. Cancer (in press)
26. Please, C.P., Pettet, G.J., McElwain, D.L.S.: A new approach to modelling the formation of necrotic regions in tumours. Appl. Math. Lett. **11**, 89–94 (1998)
27. Please, C.P., Pettet, G.J., McElwain, D.L.S.: Avascular tumour dynamics and necrosis. Math. Mod. Meth. Appl. Sci. (to appear)
28. Sherratt, J.A., Nowak, M.A.: Oncogenes, antioncogenes and the immune-response to cancer - a mathematical model. Proc. Roy. Soc. Ser. B **248**, 261–271 (1992)
29. Simon, B.R.: Multiphase poroelastic finite element models for soft tissue structures. Appl. Mech. Rev. **45**, 191–218 (1992)
30. Skalak, R., Zargaryan, S., Jain, R.K., Netti, P.A., Hoger, A.: Compatability and the genesis of residual stress by volumetric growth. J. Math. Biol. **34**, 889–914 (1996)
31. Sleeman, B.D., Nimmo, H.R.: Fluid transport in vascularized tumours and metastasis. IMA J. Math. Appl. Med. Biol. **15**, 53–63 (1997)
32. Spencer, A.J.M.: Continuum Mechanics. Longman, London, 1980
33. Sutherland, R.M., Durand, R.E.: Growth and cellular characteristics of multicell spheroids. Recent Results in Cancer Research **95**, 24–49 (1984)
34. Sutherland, R.M.: Cell and environment interactions in tumor microregions: the multicell spheroid model. Science **240**, 177–184 (1988)
35. Thompson, K.E., Byrne, H.M.: Modelling the internalisation of labelled cells in multicellular spheroids. Bull. Math. Biol. **61**, 1–23 (1999)
36. Ward, J.P., King, J.R.: Mathematical modelling of avascular tumour growth. IMA J. Math. Appl. Med. Biol. **14**, 39–69 (1997)